CrossMark

RESEARCH ARTICLE

Synthesis and Application of Novel Triazine-Based Charring-Foaming Agents in Intumescent Flame Retardant Polypropylene

Ligong Chen[1,2] · Yanyan Yuan[1,2] · Bowei Wang[1,2] · Na Liu[1,2] · Yuzhi Xing[1,2] ·
Yang Li[1,2]

Abstract Three novel triazine-based charring-foaming agents (M2-CFA, M4-CFA, and M6-CFA) were synthesized successfully with only water as the solvent and were characterized by FT-IR and thermal gravimetric analysis (TGA). These three charring-foaming agents and the byproduct 944-by were employed to study the effectiveness of the novel intumescent flame retardant dopant on the fire retardancy of polypropylene(PP) investigated through UL-94 and limiting oxygen index (LOI) tests. TGA results showed that the M4-CFA presented good char formation ability (char residue: 26.8% at 700 °C). It was found that the sample with a 2/1 mass ratio of APP to M4-CFA exhibited the best flame retardancy among all the PP composites: 35.5% LOI and a V-0 rating of UL-94. Additionally, the microstructure and morphology of char residues were further studied by XRD, Raman spectroscopy and SEM.

Keywords Triazine-based charring-foaming agent ·
Intumescent flame retardant · Thermal stability ·
Polypropylene

Introduction

As one of the most widespread polymer materials, polypropylene (PP) is used by virtue of its excellent mechanical properties, low price, low density, and superior process ability [1–3]. However, its application in electric, building, or transport industries is strongly restricted by its inherent flammability [4–6]. Therefore, flame retardation of PP has been intensively studied. Conventionally, halogenated flame retardants are effective and affordable, but there are environmental concerns with their use [6–8]. For metal hydroxides, high loadings are required to meet the flame retardant level, resulting in adverse effect on the polymer composites [9]. Hence, developing environmental friendly non-halogenated flame retardants is of considerable importance and significant interest.

Recently, intumescent flame retardant (IFR) additives have been widely utilized in the flame retardation of flammable polymers because of their advantages of being halogen-free, producing less smoke, having low toxicity, and high effectiveness [10–13]. Ammonium polyphosphate (APP), pentaerythritol (PER), and melamine (MEL) are traditional IFR components, but PER is apt to migrate to the surface due to its hydrophilic interaction and low-molecular weight, thus worsening its flame retarding efficiency [14]. To overcome these difficulties, a number of high-molecular weight charring-foaming agents (CFAs) containing triazine rings have been designed and synthesized [15]. Feng et al. [2] reported a triazine-based CFA, with 20% IFR loading, and the flame retardancy of this PP/IFR could pass a V-0 rating and reach a limiting oxygen index (LOI) for combustion of 27.1%. Su and coworkers [10] synthesized a charring agent containing a triazine ring and found that the addition of 20% IFRs into virgin PP was sufficient to reach the V-0 rating, and the LOI rose from 17.5% to 31%.

In this study, three novel triazine-based polymeric CFAs, M2-CFA, M4-CFA, and M6-CFA, were synthesized from cyanuric chloride and alkylenediamines via copolymerization. In addition, the cyclic byproduct 944-by is also

✉ Yang Li
liyang777@tju.edu.cn

1   School of Chemical Engineering and Technology, Tianjin
     University, Tianjin 300072, China

2   Collaborative Innovation Center of Chemical Science and
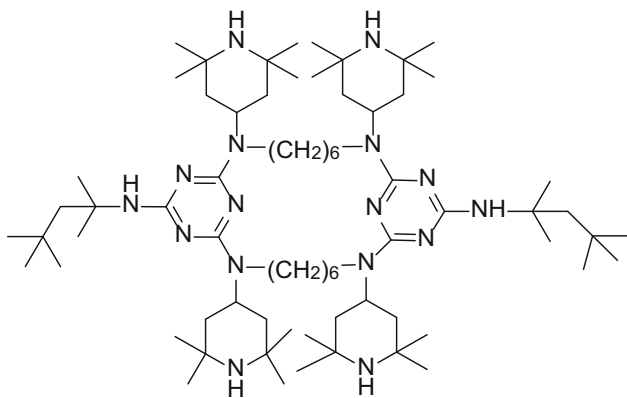   Engineering (Tianjin), Tianjin 300072, China

🙋 Springer

Fig. 1 Structure of 944-by

included in our study, which is inevitably generated in the production of Chimassorb 944 [16]; its structure is shown in Fig. 1. The behaviors of CFAs (944-by, M2-CFA, M4-CFA and M6-CFA) coordinated with APP and nano-silica on thermal degradation and flame retardancy were evaluated by thermal gravimetric analysis (TGA), LOI tests, and UL-94 tests. Moreover, the microstructures of their char residues were characterized by XRD, Raman spectra, SEM and FT-IR.

Experimental

Materials

The polypropylene in this study has a melt flow rate of 4.0 g/10 min (particles). Ammonium polyphosphate (APP, GD-APP101, phase II, degree of polymerization >1000) was obtained from Zhejiang Longyou GD Chemical Industry Co., Ltd. Nano-silica (VK-SP30S, particle size: 30 ± 5 nm) was manufactured by Ruijing New Material Co., Ltd. (Anhui, China). All raw materials used in synthesizing M2-CFA, M4-CFA, and M6-CFA, including cyanuric chloride, morphine, ethylenediamine, butanediamine, hexanediamine, sodium hydroxide, and sodium chloride, were purchased from Tianjin Guangfu Fine Chemical Research Institute. Notably, the only solvent used in this work is deionized water.

Synthesis of M2-CFA, M4-CFA, M6-CFA

A solution of morpholine (8.72 g, 100.1 mmol) in water (10 mL) and 10% NaOH aqueous solution (40 mL) were successively added into a suspension of cyanuric chloride (18.44 g, 99.8 mmol) in 3% sodium chloride aqueous solution (400 mL). The reaction mixture was stirred at 0 °C for 2 h after a precipitate appeared. It was then filtered, washed three times with water (50 mL), and dried at 50 °C in an oven to yield compound **1** (11.16 g, 95% yield). Compound **1** was a white solid with a purity of 99.7%, and its melting point was in the range of 155.2–156.7 °C, which in the literature has a melting point of 155–157 °C [17]. ^{1}H-NMR (CDCl$_3$, 400 MHz) δ: 3.90–3.88 (t, $J = 5.2$ Hz, 4H), 3.77–3.75 (t, $J = 4.4$ Hz, 4H). HRMS (ESI), calcd: $C_7H_8Cl_2N_4O$ [M+Na]$^+$ m/z: 256.9973, found: 256.9965.

Subsequently, compound **1** (23.50 g, 99.97 mmol) was suspended in water (400 mL). A mixture of ethylenediamine (7.20 g, 119.80 mmol) and NaOH (8.00 g, 200.00 mmol) in water (100 mL) was slowly added at 40 °C. Afterwards, the mixture was heated to 100 °C, refluxed for 20 h, cooled to room temperature, and then the precipitate was collected by filtration, washed three times with water (50 mL), ethanol (50 mL), and dichloromethane (50 mL), and dried at 65 °C in a vacuum oven to obtain M2-CFA (17.82 g, 90% yield) as a white solid. M4-CFA (19.57 g, 91% yield) and M6-CFA (20.65 g, 89% yield) were similarly synthesized. The synthetic routes are shown in Scheme 1.

Preparation of PP Composites

PP, APP, SiO$_2$, and CFAs (944-by, M2-CFA, M4-CFA, and M6-CFA) were dried in an oven at 105 °C overnight before use. All the samples were prepared using a two-roll mixing mill (SJSZ-8B, Wuhan, China) at 180–200 °C. In previous studies, a mass ratio of 2:1 of APP to CFA was used to prepare the PP composites [18–21]. Therefore, in this study, the ratio of APP to CFAs to SiO$_2$ was fixed at 16:8:1, and 25% IFR was blended with PP to obtain the PP composites. The detailed formulations are summarized in Table 1. Nano-silica was doped in the IFRs as a synergistic

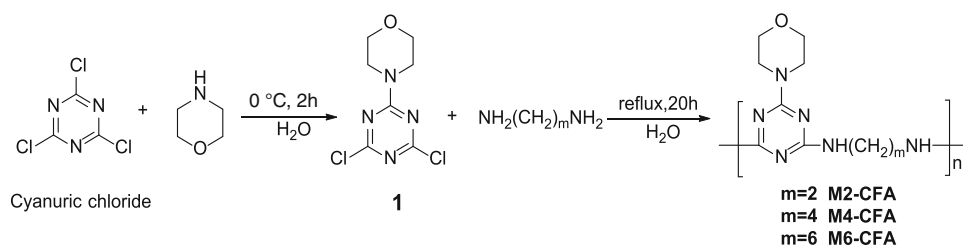**Scheme 1** Synthetic routes of M2-CFA, M4-CFA, and M6-CFA

Table 1 Effects of CFAs on flame retardancy of PP composites

Sample	CFA	Mass fraction (%)				LOI (%)	UL-94
		PP	APP	CFA	SiO$_2$		Rating
PP0	–	100	0	0	0	17.6	NR
PP1	944-by	75	16.0	8.0	1.0	24.6	NR
PP2	M2-CFA	75	16.0	8.0	1.0	31.9	V-0
PP3	M4-CFA	75	16.0	8.0	1.0	35.5	V-0
PP4	M6-CFA	75	16.0	8.0	1.0	34.3	V-0
PP5	–		24.0	0	1.0	19.0	NR

NR no rating

agent to enhance flame retardant efficiency by enhancing the mechanical strength of the char layer and by stabilizing the char layer via Si–O–P–C bonds [19, 22]. The resulting compounds were subsequently dried in an oven and then pressed on a platen press to create the required sheets for evaluation.

Characterization

^{1}H-NMR spectra were recorded on a 400 MHz ARX-300 Bruker spectrometer, using CDCl$_3$ as a solvent. FT-IR spectra were obtained with a spectrophotometer (NEXUS 670). Mass spectra were obtained using a Finnigan-4570 mass spectrometer. TGA was conducted on a Perkin Elmer Pyris1 Thermal Analyzer at a heating rate of 10 °C/min from ambient to 700 °C under an N$_2$ atmosphere. The LOI measurements were collected on a JF-3 oxygen index meter (Jiangning Analysis Instrument Company, China) with samples (130 mm × 6.5 mm × 3 mm) according to the ISO 4589-1984 standard. UL-94 tests were performed on a vertical testing apparatus (CZF-3, Jiangning Analysis Instrument Company, China) with samples (130 mm × 13 mm × 3 mm) according to the UL-94 standard. XRD was carried out using a D/MAX-2500. Laser Raman spectroscopy measurements were carried out at room temperature with a DXR Laser Raman Spectrometer. SEM was performed on an HITCHI s-4800 under an accelerating voltage of 3 kV.

To study the water resistance of PP composites, the specimens were put into distilled water at 70 °C and kept at this temperature for 168 h. The water was replaced every 24 h. The treated specimens were subsequently taken out and dried in a vacuum oven at 80 °C for 72 h, and the mass loss percentages were measured. The water resistance of the PP composites was evaluated by the change of LOI values, UL-94 ratings, and mass loss percentages.
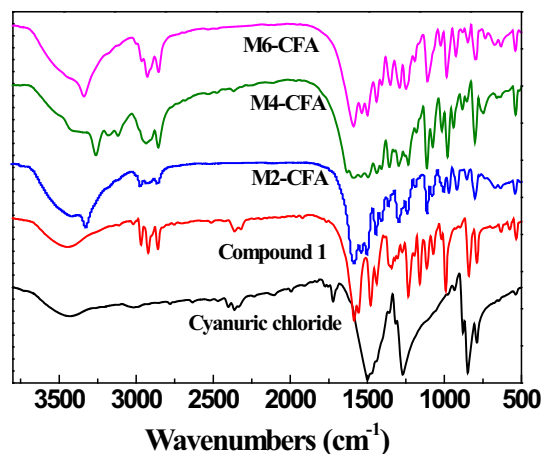

Fig. 2 FT-IR spectra of cyanuric chloride, compound **1**, M2-CFA, M4-CFA, and M6-CFA

Results and Discussion

FT-IR of Compound 1, M2-CFA, M4-CFA, and M6-CFA

As shown in Fig. 2, compared with the spectrum of cyanuric chloride, the new absorption peaks of compound **1** at 2967 and 2854 cm^{-1} can be attributed to the stretching vibration of C–H in –CH$_2$CH$_2$–, the peak at 1078 cm^{-1} corresponds to the C–O–C stretch of the morpholine ring, and the peak at 1590 cm^{-1} can be assigned to the C=N stretch of the triazine ring [15, 18]. ^{1}H-NMR (CDCl$_3$, 400 MHz) δ: 3.90–3.88 (t, J = 5.2 Hz, 4H), 3.77–3.75 (t, J = 4.4 Hz, 4H). HRMS (ESI), calcd: C$_7$H$_8$Cl$_2$N$_4$O [M+Na]$^+$ m/z: 256.9973, found: 256.9965. Therefore, it can be seen that compound **1** was successfully synthesized via the characterization by FT-IR, ^{1}H-NMR, and HRMS.

From the spectra of M2-CFA, M4-CFA and M6-CFA, the absorption bands at 3330, 3257, and 3342 cm^{-1} can be assigned to the stretching vibration of N–H of the alkylenediamine unit [20]. Thus, a conclusion can be made that M2-CFA, M4-CFA, and M6-CFA were successfully synthesized. However, it is difficult to confirm their accurate structures, because they are a mixture of insoluble compounds with different polymerization degrees [23].

Thermal Stability of CFAs and PP Composites

TGA curves of compound **1** and CFAs are shown in Fig. 3. Obviously, there are two peaks in the thermogravimetric curves of CFAs. The first one at 280–360 °C, except for 944-by at 370–410 °C, is attributed to the release of water, ammonia, and other non-flammable gases; the second peak at 410–560 °C belongs to the decomposition of CFAs [24].

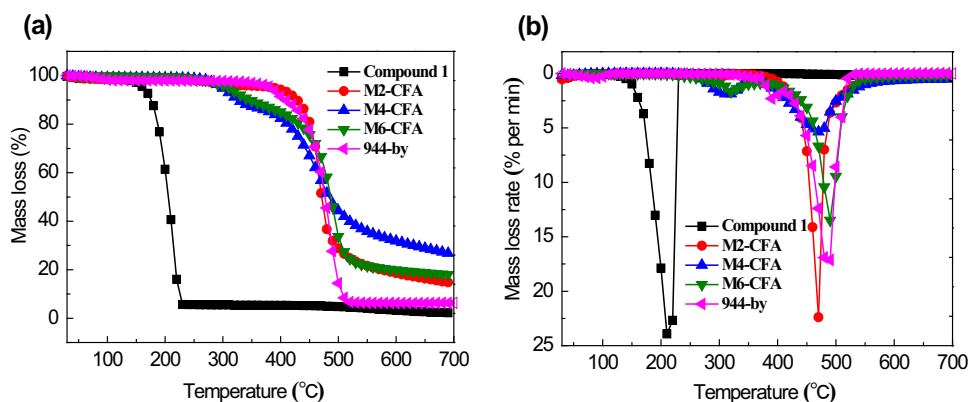**Fig. 3 a** TGA and **b** DTG curves of compound **1** and CFAs

Table 2 Thermal degradation data of compound **1** and CFAs from TGA and DTG

| Sample	$T_{initial}$ (°C)	$T_{50\%}$ (°C)	R_{peak1} (% per min)	T_{peak1} (°C)	R_{peak2} (% per min)	T_{peak2} (°C)	Char residue[a] (%)
944-by	380	477	2.31	390	17.13	490	6.31
M2-CFA	380	467	0.44	280	22.39	470	14.80
M4-CFA	290	485	1.88	310	5.37	470	26.82
M6-CFA	310	485	1.69	320	13.48	490	18.79
Compound **1**	160	204	23.93	210	–	–	2.34

[a] Char residue at 700 °C

It is obvious that M4-CFA displays the best thermal stability among the CFAs, followed by M2-CFA and M6-CFA, and 944-by has the worst thermal stability. Detailed data of the thermogravimetric analysis are presented in Table 2. The initial temperature ($T_{initial}$) represents the point when 5% of the mass is lost. Importantly, compound **1** has the lowest $T_{initial}$ of 160 °C; thus, the CFAs have markedly enhanced thermal stability over compound **1** because of copolymerization. M4-CFA was the most thermally stable among the CFAs. Its mass loss rates are 1.87% per min at 310 °C and 5.37% per min at 470 °C, and the char residues reached 26.8% at 700 °C. Thus, this shows that M4-CFA exhibits a good char formation ability.

The thermal degradation of various PP composites is shown in Fig. 4. The data are summarized in Table 3. It is seen that the virgin PP exhibits a single step of mass loss in the range of 300–480 °C, which is ascribed to the degradation of the PP backbone. The addition of APP can not only weaken the decomposition rate of PP, but also increase the char residue from 11.33 to 18.70%, which will certainly contribute to the protective effect of the degraded products of APP, such as polyphosphoric acid and polymetaphosphate. The addition of 25% IFR also improves the thermal stability of PP and increases the char residues. It is unambiguously found that the char residue of PP3 displays the highest resistance to the thermal oxidation in the high temperature range, which is confirmed by its highest char residue of 21.23%.

Flame Retardant Properties of PP Composites and Treated PP Composites

In this work, the obtained CFAs were mixed with APP and nano-silica to afford several IFRs, which were blended in PP to yield PP composites. These samples were evaluated by the LOI and UL-94 tests. The obtained results are summarized in Table 1. Pure PP is highly combustible, and cannot pass the UL-94 test. Its LOI value is only 17.6%, and its combustion presents a serious molten dripping hazard. PP5 with only 25% APP also exhibited poor anti-flaming performance and did not pass the UL-94 rating with a 19.0% LOI value. With the introduction of CFAs, the LOI of PP/IFR increased remarkably. For PP1, the LOI improved to 24.6%, which is better than pure PP; however, PP1 still did not pass the UL-94 rating, which may be associated with a low-molecular weight of 944-by.

However, as for PP2, PP3, and PP4, the LOIs were remarkably enhanced and all over 30%. As for PP3, the LOI was highest at 35.5%. Furthermore, PP2, PP3, and PP4 all reached the V-0 rating of the UL-94 tests, and the anti-dripping effect of PP was effectively improved. These results demonstrated that PP3 showed the best flame retardancy among all PP composites, followed by PP4 and PP2, and PP1 has the worst flame retardation. It is, thus, confirmed that the speculation on the thermal stability is reasonable, and the molecular weight and alkyl chain

Fig. 4 **a** TGA and **b** DTG curves of PP composites
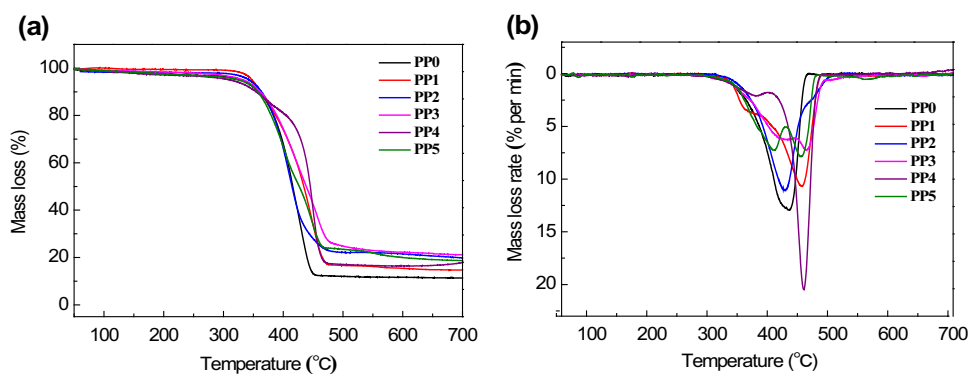
Table 3 Thermal degradation data of PP composites

Sample	$T_{initial}$ (°C)	T_{max} (°C)	R_{peak} (% per min)	Char residue[a] (%)
PP0	330	430	12.94	11.33
PP1	347	448	10.68	14.73
PP2	340	422	11.10	20.71
PP3	331	456	7.23	21.23
PP4	310	452	20.47	17.75
PP5	324	447	7.86	18.70

[a] Char residue at 700 °C

length of diamines do impact the flame retardancy of CFAs.

Photographs of PP0, PP1, PP2, PP3, PP4, and PP5 specimens after LOI tests are shown in Fig. 5. It can be seen that PP0 and PP5 both are in a melted form without obvious char residues; however, char residues are observed for PP1, PP2, PP3, and PP4 specimens. Compared to PP2, PP3, and PP4, the char layer of PP1 is very thin and not effective at preventing the combustion of the underlying resins. In addition, melt drippings were observed during the PP1 tests. In contrast, PP3 produced more char residue than PP2 and PP4, which is consistent with the results of the flame retardant tests.

The flame retardancy of the treated PP composites was also studied by the LOI and UL-94 burning tests. As revealed in Table 4, the LOIs of the treated PP composites are slightly reduced. Among all the samples, the LOI of PP3 decreased the least. Meanwhile, PP2, PP3, and PP4 still successfully passed the UL-94 V-0 rating. Furthermore, the water resistance of PP2, PP3, and PP4 was excellent due to the hydrophobicity of synthesized M2-CFA, M4-CFA, and M6-CFA. Among treated PP composites, PP3 presented the best water resistance.

Microstructure Analysis of the Residual Char

The microstructure of the residual char is very important to the flame retardant properties of the polymer. For an IFR-doped polymer system, the graphitization degree of char is a very critical structural parameter, which reflects the transition extent of carbon materials from a turbostratic structure to graphitic structure, which determines the properties of the char [25]. Thus, XRD and Raman spectroscopy were employed to further characterize the graphitization degree of the residual char here [26].

XRD

The (002) peak in the XRD profile is a reflection of all the micrographite crystals in the carbon materials. According to the Bragg Eq. ($2d\sin\theta = n\lambda$), the interlayer spacing $d_{(002)}$ can be derived from the diffraction angle (θ) of the (002) peak. Combining this with Eq. (1) below, the value of the graphitization degree (g) can be calculated.

$$g\% = \frac{0.3440 - d_{(002)}}{0.3440 - 0.3354} \times 100\% \tag{1}$$

Such an equation has its limitation; in fact, at times $d_{(002)}$ is greater than 0.3440 nm. Therefore, it is only used in this paper to show that we have a structure that is far from the ideal graphite structure [25].

XRD profiles of the PP residues after LOI tests are presented in Fig. 6a. Related data are presented in Table 5. The $d_{(002)}$ values of the char residues of PP1 and PP3 are both 0.3624 nm, which are larger than the perfect graphite distance of 0.3440 nm, whereas PP2 was the largest at 0.4244 nm. Combined with the effects of CFAs on flame retardancy of IFR-PP systems (Table 1), it can be further
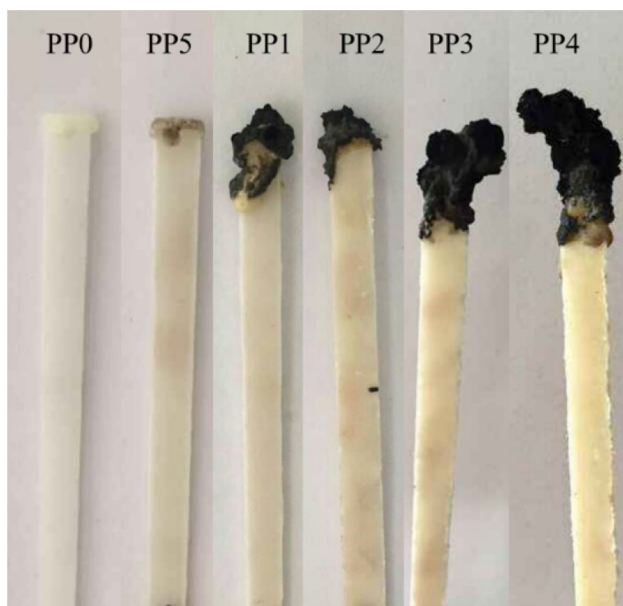
Fig. 5 Digital photographs of specimens after LOI tests

Table 4 The flame retardancy of treated PP composites

Sample no.	Mass loss percentage (%)	UL-94	LOI (%)	ΔLOI (%)
PP2	0.44	V-0	31.0	−0.9
PP3	0.25	V-0	35.1	−0.4
PP4	0.65	V-0	33.2	−1.1
PP5	6.44	NR	18.1	−0.9

verified that PP3 exhibited better flammability properties on account of the formation of a sufficient and desirable char layer, and PP1 was not ideal on account of the little char residue in spite of the favorable char microstructure. Therefore, both quality (graphitization degree) and quantity of the char residue are the indispensable parameters to study the flammability properties of the polymers.

Raman Spectra

Raman spectroscopy has been increasingly employed as an effective technique to evaluate the graphitization degree of char [26, 27]. Raman spectra of the residues after LOI tests are presented in Fig. 6b. Obviously, the peak at 1600 cm^{-1} (G-band) corresponds to an E_{2g} mode of the hexagonal graphite layer, and the peak at about 1380 cm^{-1} (D-band) is associated with the vibration of carbon atoms with dangling bonds in the plane terminations of disordered graphite or glassy carbon [28, 29]. The ratio of the integral peak intensity of the D-band and G-band, $R = I_D/I_G$, represents the graphitization degree of the chars [7]. The integrated results are shown in Table 5. It is found that the R values of PP1, PP3, and PP4 were 1.51, 2.64, and 2.67, respectively, while PP2 was 3.27. Thus, this illustrates that PP1, PP3, and PP4 form a char layer of high graphitization degree, which is consistent with the XRD results. However, by the result of Table 1, PP1 shows a poor flame retardant property because the char residue was insufficient to protect the underlying materials. Nevertheless, the flammability of PP3 remains the desirable formulation.

Fig. 6 a XRD profile and b Raman spectra of the residues of PP1, PP2, PP3, and PP4 after LOI tests
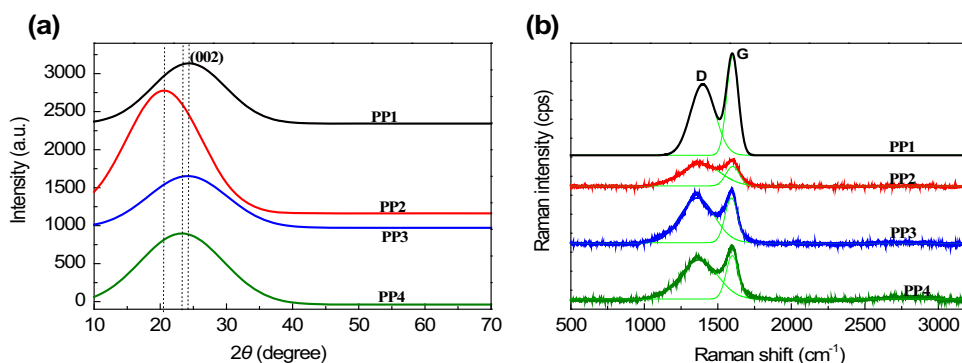
Table 5 XRD and Raman analysis data of char residues for PP1, PP2, PP3, and PP4
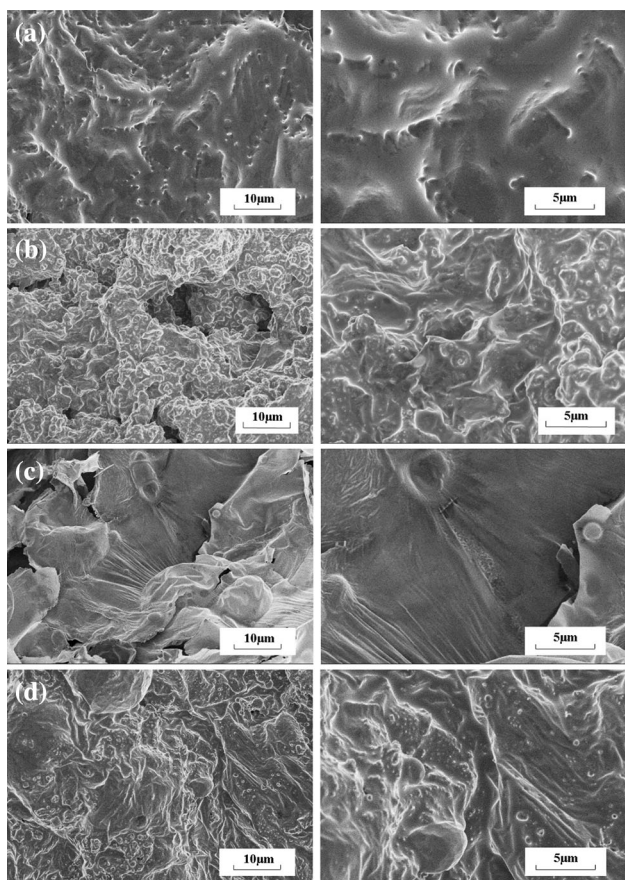
Sample	XRD			Raman		
	2θ (°)	$d_{(002)}$	d_0	I_D	I_G	$R = I_D/I_G$
PP1	24.54	0.3624	0.3354	19494.43	12937.18	1.51
PP2	20.91	0.4244		9674.09	2962.60	3.27
PP3	24.54	0.3624		16965.13	6421.08	2.64
PP4	23.33	0.3809		16226.40	6016.61	2.67

d_0: 0.3354 nm is the interlayer spacing of the ideal graphite crystallite

Fig. 7 SEM micrographs of the residual chars of **a** PP1, **b** PP2, **c** PP3, and **d** PP4

SEM

To further illustrate the effects of CFAs on PP composites, the morphology of the residual chars after the LOI tests was analyzed by SEM. As shown in Fig. 7, for PP1 and PP2, some cracks and obvious holes can be observed on the accidented surface of the residue due to insufficient char formation during combustion. In contrast, the char layers of PP3 and PP4 are intact, compact, and continuous, which effectively prevent the transfer of heat, mass, and flammable volatiles, and they also prevent the generation of molten drops, thereby leading to better flame retardancy [12]. It was indicated that poor char layers of PP1 and PP2 formed after combustion resulted in undesirable flame retardancy [30]. These SEM results further showed that PP3 and PP4 displayed better flame retardant properties than PP1 and PP2. Finally, it is, thus, clearly verified that the molecular weight and alkyl chain length of diamines play key roles in the flame retardancy of CFAs.

Component Analysis of the Final Char

The chemical components of the char residues of PP composites after the LOI tests were investigated by FT-IR.
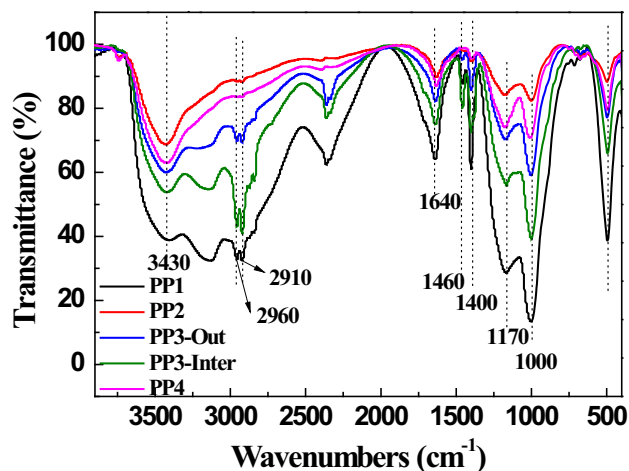

Fig. 8 FT-IR spectra of the residues for PP1, PP2, PP3-Out, PP3-Inter, and PP4

The profiles are presented in Fig. 8. The peaks at 3430 and 1640 cm^{-1} are assigned to the stretching modes of N–H in NH_4^+ and of C=C in polyaromatics, respectively [22]. The peaks at 1400, 1170, and 1000 cm^{-1} correspond to the stretching vibration of P–N, Si–O, and P–O. It was shown that cross-linking reactions among CFAs, APP, and SiO_2 formed aromatic and phosphorous char layers during combustion that act as powerful flame shields to protect the underlying materials from further degradation [7, 10]. The characteristic peaks appear at 2960 and 2910 cm^{-1} in the curves of PP1, PP3-Out, and PP3-Inter, which belong to the absorption by C–H bonds [12, 20]. The peaks clearly confirmed that PP1 and PP3 were not burnt completely, and suggest that chemical synergistic effects in PP1 or PP3 could further enhance self-charring ability [1]. However, based on the flame retardancy of the PP composites, despite a high graphitization degree of the char, PP1 has poor flammability due to the thin char layer. Whereas, PP3 displayed the best flame retardancy, which correlates with the good thermal stability of M4-CFA.

Based on the results of TGA, LOI tests, UL-94, XRD, Raman spectroscopy, and SEM tests, it is found that there exists a synergistic effect between APP and CFAs in the process of combustion. During thermal decomposition, firstly, APP decomposes and evolves both water and ammonia to form phosphoric acid at about 300 °C. Then, the reaction between the phosphoric acid and CFA generates a phosphate ester. The gases, which were produced during the first two processes, cause the swelling of PP. When the temperature continues to rise, CFA begins to dehydrate and react with the derived acid from the decomposition of APP. Meanwhile, the ester performs cyclization and crosslinking, resulting in the formation of an intumescent char of the PP composites. CFAs combined with APP promote the accumulation and formation of a

phosphoritic and aromatic char possessing a high degree of graphitization.

From our study, it is speculated that the highest char yield of M4-CFA might be connected with the structure of monomer-butanediamine. Generally, it is too complicated to analyze the structure of a polymer such as this [1, 2]. However, we have confirmed that the CFAs with different alkyl chain lengths have a great influence on PP composites, indicating that a suitable length of alkyl chains should be selected to synthesize CFAs. This is important for the design and preparation of more efficient CFAs.

Conclusions

In this study, three novel triazine-based charring-foaming agents (M2-CFA, M4-CFA, and M6-CFA) were synthesized successfully with water as the sole solvent. These three charring-foaming agents and 944-by were employed to study the effects of CFAs on the flame retardancy of PP composites. PP1 showed the worst flame retardancy due to its low self-charring ability. However, PP3 with a 2/1 mass ratio of APP to M4-CFA displayed the best flame retardancy among all PP composites. The LOI was 35.5%, and the UL-94 rating passed V-0. The superior performance of PP3 is ascribed to the good thermal stability of M4-CFA and formation of a sufficiently thick char residue that is intumescent, compact, and has a high graphitization degree. Furthermore, PP2 and PP4 also showed better flame retardancy than PP1, but not as good as PP3. The LOIs of PP2 and PP4 were 31.9 and 34.3%, respectively, and they passed the V-0 rating. The microstructure, morphology, and components of char residues were further studied by XRD, Raman spectroscopy, and SEM. The results indicate that PP3 could form a high graphitization degree aromatic char layer containing P–O–C and P–N bonds during the combustion process. As a general conclusion, diverse flame retardancy among PP2, PP3, and PP4 stems from the CFAs with different alkyl chain lengths of diamines, indicating that CFAs with different alkyl chain lengths have a great influence on PP composites.

References

1. Wen PY, Wang XF, Wang BB et al (2014) One-pot synthesis of a novel-s-triazine-based hyperbranched charring foaming agent and its enhancement on flame retardancy and water resistance of polypropylene. Polym Degrad Stab 110:165–174
2. Feng CM, Zhang Y, Liu SW et al (2012) Synthesis of novel triazine charring agent and its effect in intumescent flame-retardant polypropylene. J Appl Polym Sci 123(6):3208–3216
3. Chen SJ, Li J, Zhu YK et al (2013) Increasing the efficiency of intumescent flame retardant polypropylene catalyzed by polyoxometalate based ionic liquid. J Mater Chem A 1(48):15242–15246
4. Feng Y, Tang WW, Huang YY et al (2014) (Solid +(plus) liquid) phase equilibria of tetraphenyl piperazine-1,4-diyldiphosphonate in pure solvents. J Chem Thermodyn 78:143–151
5. Feng Y, Dai H, Gao WS et al (2015) Measurement and correlation of solubility of tetraphenyl piperazine-1,4-diyldiphosphonate in mixed solvents. J Chem Eng Data 60(3):561–567
6. Wang DY, Cai XX, Qu MH et al (2008) Preparation and flammability of a novel intumescent flame-retardant poly (ethylene-co-vinyl acetate) system. Polym Degrad Stab 93(12):2186–2192
7. You GY, Cheng ZQ, Peng H et al (2014) The synthesis and characterization of a novel phosphorus-Nitrogen containing flame retardant and its application in epoxy resins. J Appl Polym Sci 131(22):547–557
8. Liu JC, Yu ZL, Shi YZ et al (2014) A preliminary study on the thermal degradation behavior and flame retardancy of high impact polystyrene/magnesium hydroxide/microencapsulated red phosphorus composite with a gradient structure. Polym Degrad Stab 105(1):21–30
9. Xing WY, Song L, Lu HD et al (2009) Flame retardancy and thermal degradation of intumescent flame retardant polypropylene with MP/TPMP. Polym Adv Technol 20(8):696–702
10. Su XQ, Yi YW, Tao J et al (2014) Synergistic effect between a novel triazine charring agent and ammonium polyphosphate on flame retardancy and thermal behavior of polypropylene. Polym Degrad Stab 105(1):12–20
11. Li HX, Ning NY, Zhang LQ et al (2014) Different flame retardancy effects and mechanisms of aluminium phosphinate in PPO, TPU and PP. Polym Degrad Stab 105(7):86–95
12. Xie F, Wang YZ, Yang B et al (2006) A novel intumescent flame-retardant polyethylene system. Macromol Mater Eng 291(3):247–253
13. Wang JJ, Ren Q, Zheng WG et al (2014) Improved flame-retardant properties of poly (lactic acid) foams using starch as a natural charring agent. Ind Eng Chem Res 53(4):1422–1430
14. Enescu D, Frache A, Lavaselli M et al (2013) Novel phosphorous-nitrogen intumescent flame retardant system. Its effects on flame retardancy and thermal properties of polypropylene. Polym Degrad Stab 98(1):297–305
15. Feng CM, Li ZW, Liang MY et al (2015) Preparation and characterization of a novel oligomeric charring agent and its application in halogen-free flame retardant polypropylene. J Anal Appl Pyrol 111:238–246
16. Cantatore Giuseppe. Piperidyl derivatives of triazine copolymers, processes for their preparation and stabilized composition containing these derivatives: US, 4,459,395. 1984-07-10
17. Braun D, Ghahary R, Ziser T (1995) Triazine-based polymers, 3. synthesis and characterization of polyamines. Die Angewandte Makromolekulare Chemie 233(1):121–131
18. Zhan J, Song L, Nie SB et al (2009) Combustion properties and thermal degradation behavior of polylactide with an effective intumescent flame retardant. Polym Degrad Stab 94(3):291–296
19. Li B, Xu MJ (2006) Effect of a novel charring-foaming agent on flame retardancy and thermal degradation of intumescent flame retardant polypropylene. Polym Degrad Stab 91(6):1380–1386
20. Yang K, Xu MJ, Li B (2013) Synthesis of N-ethyl triazine-piperazine copolymer and flame retardancy and water resistance of intumescent flame retardant polypropylene. Polym Degrad Stab 98(7):1397–1406
21. Wen PY, Wang XF, Xing WY et al (2013) Synthesis of a novel triazine-based hyperbranched char foaming agent and the study of its enhancement on flame retardancy and thermal stability of polypropylene. Ind Eng Chem Res 52(48):17015–17022
22. Deng CL, Du SL, Zhao J et al (2014) An intumescent flame retardant polypropylene system with simultaneously improved

flame retardancy and water resistance. Polym Degrad Stab 108:97–107

23. Han JP, Liang GZ, Gu AJ et al (2013) A novel inorganic-organic hybridized intumescent flame retardant and its super flame retarding cyanate ester resins. J Mater Chem A 1(6):2169–2182

24. Yi JS, Liu Y, Pan DD et al (2013) Synthesis, thermal degradation, and flame retardancy of a novel charring agent aliphatic—aromatic polyamide for intumescent flame retardant polypropylene. J Appl Polym Sci 127(2):1061–1068

25. Ma HY, Fang ZP (2012) Synthesis and carbonization chemistry of a phosphorous-nitrogen based intumescent flame retardant. Thermochim Acta 543:130–136

26. Zou LH, Huang BY, Huang Y et al (2003) An investigation of heterogeneity of the degree of graphitization in carbon-carbon composites. Mater Chem Phys 82(3):654–662

27. Centeno A, Blanco C, Santamaria R et al (2012) Further studies on the use of Raman spectroscopy and X-ray diffraction for the characterization of TiC-containing carbon-carbon composites. Carbon 50(9):3240–3246

28. Sheng CD (2007) Char structure characterized by Raman spectroscopy and its correlations with combustion reactivity. Fuel 86(15):2316–2324

29. Wang Y, Alsmeyer DC, Richard LM (1990) Raman spectroscopy of carbon material: structural basis of observed spectra. Chem Mater 2(5):557–563

30. Shao ZB, Deng C, Tan Y et al (2014) Ammonium polyphosphate chemically-modified with ethanolamine as an efficient intumescent flame retardant for polypropylene. J Mater Chem A 2(34):13955–13965